اونيۏرسيتي مليسيا ڤهڠ
UNIVERSITI MALAYSIA PAHANG

ORIGINAL ARTICLE

Development of Lab Scale MAVeP Mobility Prototype

M.A. Abd Mutalib[1] and N. Zainul Azlan[2,*]

[1]Machine Design Section, Machinery Technology Centre, SIRIM Berhad. Lot 1A, Persiaran Zurah, Kawasan Perindustrian Rasa, 44200 Rasa, Selangor, Malaysia
[2]Department of Mechatronics Engineering, Kuliyyah of Engineering, International Islamic University Malaysia, 53100 Gombak, Malaysia

ABSTRACT – This paper presents the development, calibration and mechanism control of lab scale Motorised Adjustable Vertical Platform (MAVeP) mobility prototype. MAVeP has been developed and equipped with mecanum wheels to allow an omnidirectional movement. The omnidirectionality, or the ability to move in any direction, without altering the direction of the MAVeP's body, makes this type of driving useful, especially in narrow and confined areas such as inside satellite assembly, integration and test centre (AITC). Since MAVeP has been delivered at AITC and high accuracy and repeatability movement are crucial during the application, a robot prototype representing MAVeP mobility has been designed and developed. The mechanical and electrical design, including all processes and components, are selected and explained in detail. The development of the robot prototype, its parameters and calibration are also discussed. The DC motor control for separate wheels of the MAVeP mobility prototype using PID controller and the calibrations to synchronous the four wheels' rotation are also discussed in this paper. The experimental result shows that the robot prototype is established and ready to be used in research.

INTRODUCTION

Wheeled machine-like mobile robot is becoming popular and widely used in industries for automated transportation or logistic purposes such as carrying goods, parts and even people. While dealing with an expensive and sensitive load, the mobile robot needs to be reliable, safe and provide efficient movements. A machine with its own wheels is able to move around and make its usage more efficient. Mobile robots can serve at more than one station in the production line at the same time can increase the capacity and quality of products. However, to drive a machine in a confined area where the movement is restricted is a big challenge. In this circumstance, a more effective driving method is necessary and therefore, omnidirectional driving can full fill the need. The usage of mecanum wheels enables the machine to be driven in omnidirectional where it can move in any direction without altering the direction of the mobile robot's body.

The mecanum wheel provides special omnidirectional manoeuvrability and has been utilized in various applications. For example, the high degree of manoeuvrability has been utilized by NASA in the development of their OnmiBot. OmniBot is used in the exploration of hazardous environments where it is too dangerous for unprotected personnel. The OmniBot is equipped with mecanum wheels to allow it to perform the complete 2-degree-of-freedom motions for site survey, remote inspection and operation [1].

Meanwhile, in the transportation industries, Satellite Systems Corporation has developed a forklift names Airtrax ATX-3000, equipped with mecanum wheels. This forklift is designed to accomplish the requirement of tight manoeuvring or transporting lengthy loads in a sideway manner to pass through standard door size or narrow walkways. Since the application is heavy, the mecanum wheel rollers are designed with a heavy-duty hub and 12 polyurethane rollers. The rollers are integrated with special bearings that do not require periodic greasing and create free maintenance conditions. Since each roller rotates freely, the roller`s pressure against the floor is low during turning or moving sideways. The speed and direction of manoeuvring are controlled by joysticks [2].

Mecanum wheels can also be equipped with shopping carts. The cart, Interactive Behaviour Operated Trolley (InBOT) provides a comfortable shopping experience for the customer in getting their items, especially in the huge supermarket, by relieving the burden of pushing the ordinary shopping cart. InBOT has been embedded with a collision avoidance function. There are four different functions of InBOT operation available in assisting the users; it steers like an ordinary shopping cart with a haptic handle but comes with an obstacle avoidance function, follows the user, leads the user, and the most advanced function is commanded to act independently until ordered otherwise [3].

Besides carrying goods, mecanum wheels are also studied to carry humans. It has been assembled into wheelchairs to improve the elderly`s quality of life where they are decreased in ability to walk and do not have the strength, stamina, or ability to move the manual wheelchair by themselves. The Office Wheelchair for High Manoeuvrability and Navigational Intelligence for People with Severe Handicap (OMNI) has been developed at the University of Western Australia's Centre for Intelligent Information Processing Systems (CIIPS). It provides three degrees of freedom (3-DOF) manoeuvrability. It comes with a joystick, infrared (IR) and ultrasound sensors for obstacle detection, a bumper sensor for collision detection, an odometer and an elevating seat for users' convenience [4].

Since mecanum wheels have been proven to be reliable and applicable for enabling mobile robot applications, a motorized adjustable vertical platform (MAVeP) has been designed and equipped with mecanum wheels for mobility. MAVeP has been designed and developed to replace a standard mechanical ground support equipment (MGSE) trolley, or called multi-purpose satellite trolleys offered at most of the test centre, which is not suitable to be used AITC in terms of mobility and height. During the test procedures, a mobile trolley is required to transport the satellite to several test areas and allows an engineer to do their assimilation work at a few parts of the satellite body in order to set up the satellite for the test. The MAVeP's application requires a smooth and easy operation as well as low handling risk that may jeopardize the satellite test result. The MAVeP`s also equipped with automatic mobility control and adjustable height to elevate the satellite according to Agensi Angkasa Malaysia (MYSA) requirement [5].

The MAVeP`s is required to move very accurate, especially in front of the TVC where auto parking mode is enabled. The parking tolerance is only 2 cm, before the satellite can start to be lifted. The construction of the mecanum wheel itself consists of a free roller. This creates difficulties to park the MAVeP accurately with good repeatability. The free roller leads to slippage phenomena. The slippage issue cannot be eliminated unless the construction of the wheel is enhanced. Besides, the huge MAVeP`s of 6000 kg weight requires high torque of motors to carry the load. This leads to vibration and jerking during the movement. To resolve those issues, a MAVeP mobility prototype has been developed to further understand wheeled machine-like robot behaviours in terms of movements, e.g. accuracy, transient response, effect to load, friction, slippage and controller development [6].

This paper presents the design and development of MAVeP mobility prototype in mechanical and electrical aspects to be used in our future research. The process of designing and preparing of MAVeP mobility prototype is discussed in the Design and Fabrication of Lab Scale MAVeP Mobility Prototype section. Motions and interaction are explained in Kinematic Analysis and Dynamic Modelling. DC motor used as actuator explains the reason of actuator and controller selection including its parameter and basic position controller including the calibration steps before MAVeP mobility hardware is fully tested.

DESIGN AND FABRICATION OF LAB SCALE MAVEP MOBILITY PROTOTYPE

A basic prototype of MAVeP mobility has been developed as a platform for experimental work in WISE laboratory, International Islamic University Malaysia (IIUM) [6]. Figure 1 shows the control block diagram of the designed MAVeP mobility prototype. Figure 2 shows the system architecture. W1, W2, W3 and W4 refer to wheel 1, wheel 2, wheel 3 and wheel 4 respectively. There are three units of ultrasonic distance sensors attached to MAVeP mobility prototype; two units in front and one unit on the left. Both sensor readings at the front side; Sensor 1 and Sensor 2 are compared to each other to ensure that the robot prototype moves in a straight path. A slight divergence between those readings indicates that the mobile robot prototype is not moving straight. The ultrasonic distance sensor is located on the left side; Sensor 3 defines the sideways movement.
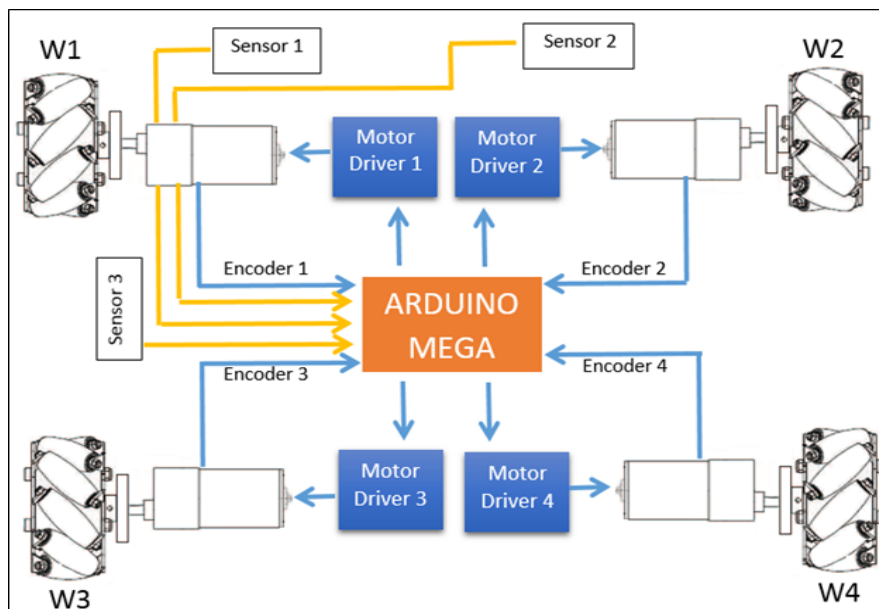
Figure 1. MAVeP mobility prototype block diagram.
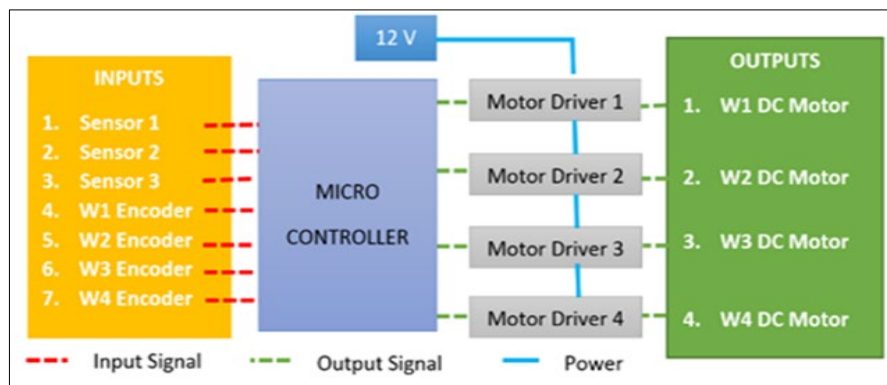
Figure 2. MAVeP Mobility prototype control system architecture.

As per the requirement of mecanum wheels system, each wheel is driven individually. For this prototype, DC motors has been selected to be used as the actuator since it is good in speed control. In order to control the movements of MAVeP mobility prototype, the motor rotation needs to be measured. All four motors are equipped with rotary encoders. For convenience, the developed prototype is powered by a 12V battery which is suitable for the mobile robot`s application. Arduino Mega microcontroller has been selected as the hardware controller since it has six pulse width modulator (PWM) pins outputs, and six interrupt pins for encoder reading. These types of controller were also used in [7],[8] and [9]. The price is also reasonable compared to other types of the microcontroller which are available in the market.

Table 1 shows the list of finalized components that have been used in the development of MAVeP mobility prototype. Since our future research requires a high precision and accuracy movement of the prototype, the mechanical part development has gone through standard fabrication processes, including modelling, machining and fitting before completing the assembly. Since the prototype represents the real MAVeP mobility, the development has to be scaled. Figure 3 shows the comparison of MAVeP mobility prototype mecanum wheel to the real MAVeP mecanum wheel. Since the mecanum wheel used for the MAVeP mobility prototype is a standard part available in the market, the scaling factor is 457 mm / 30 mm or 15.23. Figure 4 shows the dimension of MAVeP. From Figure 4, the MAVeP has been designed with 4000 mm long and 3500 mm in width. After calculating with 15.23 factor, the size of the prototype must be 262.6 mm ~ 263mm long and 229.8mm ~230mm in width. Figure 5(a) shows the main structure of the MAVeP mobility prototype design details.

Table 1. MAVeP mobility prototype equipment.

Components	Model number	Quantity
Mecanum wheel	CYT3626	4
DC motor with encoder	SPG30E-60K	4
Motor driver	MD10C	4
Motor holder	SD-SS-10	4
Arduino mega	2560 Rev 3	1
Distance sensor	US-100	3
12V Battery	LIP-11,1500	1
Charger	LIP-CRB6AC	1
Voltage regulator	LM78051C	1
Bread board	BD-BB-0617	1
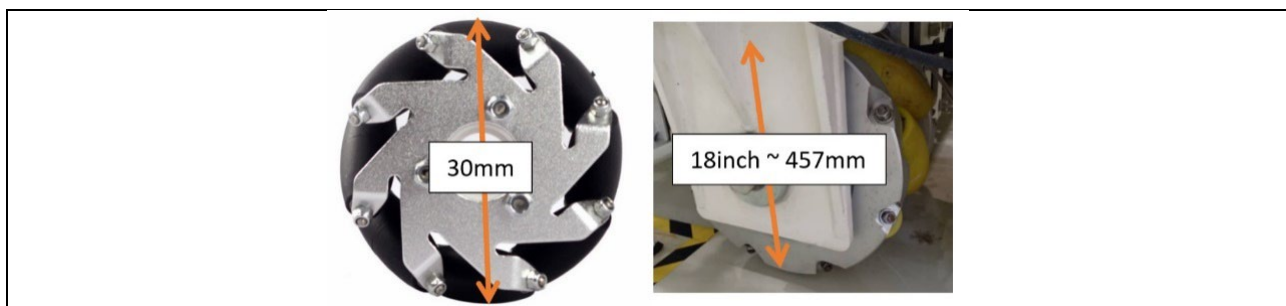
Figure 3. Comparison of MAVeP mobility prototype mecanum wheel to real MAVeP mecanum wheel.

To come out with the structure design as shown in Figure 5(a), the design started with the modelling. All the equipment involved needs to be modelled and assembled. As a result, the designer will know the location of the holes and every single screw required. The designer shall come out with the bill of quantity (BOQ) of the designed MAVeP mobility prototype after this step. Figure 5(b) shows the isometric view of MAVeP mobility prototype modelling process.

Figure 4. MAVeP dimensions.

(a)   (b)
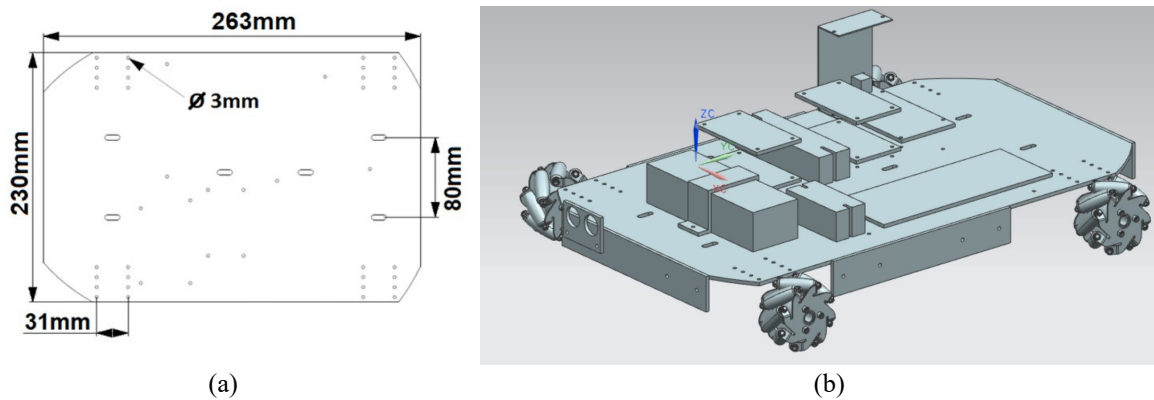
Figure 5. (a) Main structure design and (b) isometric view of MAVeP mobility prototype.

The mechanical work at this point is the stage of fabrication. A mild steel plate with 3 mm thickness has been verified to be rigid enough to be used for the MAVeP mobility prototype-based structure. To ensure the cutting accuracy, the plate was cut using a laser cutting machine. Figure 6(a) shows the laser cutting process, while Figure 6(b) shows the parts after the laser cutting. The metal work is not complete without a welding process. To complete the fabrication, the parts have been assembled by welding. The sensor bracket has been welded to the main structure. Even though the sensor is only located in front and at the left side, the brackets are welded to all sides. This bracket is used to prevent the main structure from the bend and increase its stiffness. Finally, the fabrication process is finished with deburring. Figure 6(c) shows the deburring process by using a hand grinder.

Next, the mechanical development is continued with the fitting process. Some people call this step as pre-assembled. Fitting process is very important and sometimes is ignored. Machining and fabrication processes have their own accepted tolerances and cannot be hundred percent accurate. Similarly, for this prototype, some of the holes need to be modified after the machining process. The fitting step can avoid any modification after the painting process. Figure 7 shows the fitting process during the MAVeP mobility prototype development. After the required modification, the structure has been disassembled and continued with painting works. Painting work is important for all metal works. Not only it makes the prototype looks neat, the painting can also protect the prototype from becoming rusty. The electronics parts also will be affected if the main structure is rusty. Figure 8 shows the main prototype structure painting work. The final process is the assembly work. Since the structure has gone through the fitting process, the assembly work is not tough, especially for prototype development. The wiring process has also been carried out. Figure 9 shows the MAVeP mobility prototype is ready to be used for hardware experimental tests.

(a)   (b)   (c)
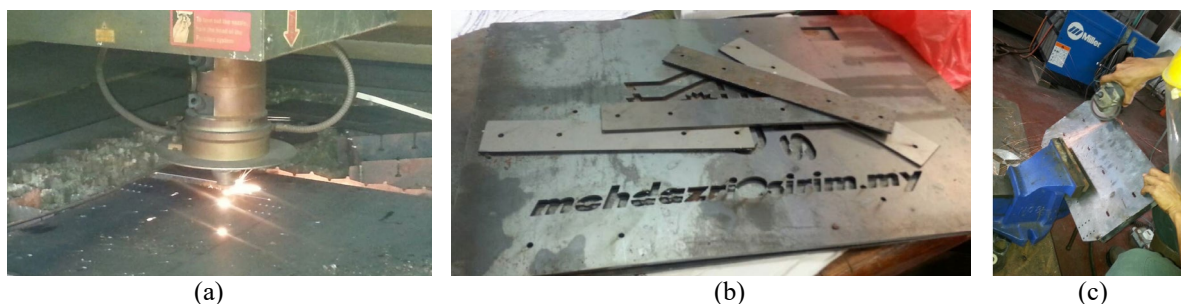
Figure 6. (a) Laser cutting process, (b) parts after laser cutting process, and (c) deburring process using a hand grinder.

Figure 7. MAVeP mobility prototype fitting process.

Figure 8. MAVeP mobility prototype main structure paintwork.

Figure 9. MAVeP mobility prototype.

KINEMATIC ANALYSIS AND DYNAMIC MODELLING

Kinematic Analysis

Kinematic is a study of object in motion and their inter-relationship related to displacement, velocity, acceleration and time[9]. For MAVeP mobility prototype, the kinematic equation is derived from a single mecanum wheel; the final equation is representing four mecanum wheels used. Figure 10 shows the free body diagram of MAVeP mobility prototype.

Referring to Figure 10, $\omega_i (i = 1,2,3,4)$ is the angular velocity of the wheel. Assuming there is no slippage, the velocity vector of MAVeP mobility prototype corresponding to the wheels' angular velocity is $V_{\omega i} = R \times \omega_i$, R is the radius of wheels. $r_i (i = 1,2,3,4)$ is the tangent to the free roller and represents the direction of the free roller rotation. The velocity vector of the free roller contacts the floor is $V_{ri} (i = 1,2,3,4)$ and the angle is 45° since the MAVeP is using a conventional mecanum wheel.

For linear movement, the velocity with respect to X direction is $V_{iX} (i = 1,2,3,4)$ derived from the wheel velocity $V_{\omega i}$ and V_{ri} x cos 45°. For the velocity with respect to Y direction is $V_{iY} (i = 1,2,3,4)$ also derived from V_{ri} x sin 45°. The value of sin 45° and cos 45° used here is $1/\sqrt{2}$. Therefore;

$$V_{1X} = V_{\omega 1} + \frac{V_{r1}}{\sqrt{2}} \quad , \qquad V_{1Y} = \frac{V_{r1}}{\sqrt{2}} \tag{1}$$

$$V_{2X} = V_{\omega 2} + \frac{V_{r2}}{\sqrt{2}}, \qquad V_{2Y} = \frac{V_{r2}}{\sqrt{2}} \tag{2}$$

$$V_{3X} = V_{\omega 3} + \frac{V_{r3}}{\sqrt{2}} \quad , \qquad V_{3Y} = \frac{V_{r3}}{\sqrt{2}} \qquad (3)$$

$$V_{4X} = V_{\omega 4} + \frac{V_{r4}}{\sqrt{2}} \quad , \qquad V_{4Y} = \frac{V_{r4}}{\sqrt{2}} \qquad (4)$$

The rotational movement is derived from MAVeP mobility prototype velocity direction to X axis; V_X, Y axis; V_Y and rotational C axis; V_C. $V_{iX}(i = 1,2,3,4)$ is equal to V_X plus the distance of the wheel centre to the platform in X direction times V_C and $V_{iY}(i = 1,2,3,4)$ is equal to V_Y plus the distance of the wheel centre to the platform in Y direction times V_C.

$$V_{1X} = V_X + (-W\ V_C), \qquad V_{1Y} = V_Y + LV_C \qquad (5)$$

$$V_{2X} = V_X + W\ V_C, \quad V_{2Y} = V_Y + LV_C \qquad (6)$$

$$V_{3X} = V_X + (-W\ V_C), \qquad V_{3Y} = V_Y + (-LV_C\ ) \qquad (7)$$

$$V_{4X} = V_X + W\ V_C\ , \qquad V_{4Y} = V_Y + (-LV_C\ ) \qquad (8)$$
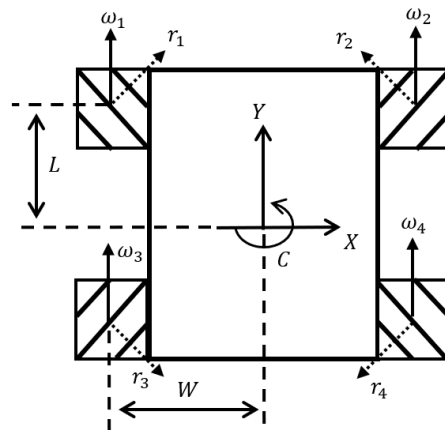
Figure 10. MAVeP mobility prototype free body diagram.

After simplifying Eq. (1) to Eq. (8), the following equations are obtained;

$$V_{\omega 1} = V_X - V_Y - (L + W)\ V_C \qquad (9)$$

$$V_{\omega 2} = V_X + V_Y + (L + W)\ V_C \qquad (10)$$

$$V_{\omega 3} = V_X + V_Y - (L + W)\ V_C \qquad (11)$$

$$V_{\omega 4} = V_X - V_Y + (L + W)\ V_C \qquad (12)$$

Equation (9) to Eq. (12) can be written in matrix form as;

$$\begin{bmatrix} V_{\omega 1} \\ V_{\omega 2} \\ V_{\omega 3} \\ V_{\omega 4} \end{bmatrix} = \begin{bmatrix} 1 & -1 & -(L+W) \\ 1 & 1 & (L+W) \\ 1 & 1 & -(L+W) \\ 1 & -1 & (L+W) \end{bmatrix} \begin{bmatrix} V_X \\ V_Y \\ V_C \end{bmatrix} \qquad (13)$$

Since $V_{\omega i} = R \times \omega_i$ and R is identical to all four wheels;

$$\begin{bmatrix} V_{\omega 1} \\ V_{\omega 2} \\ V_{\omega 3} \\ V_{\omega 4} \end{bmatrix} = \begin{bmatrix} R\ \omega_1 \\ R\ \omega_2 \\ R\ \omega_3 \\ R\ \omega_4 \end{bmatrix} \qquad (14)$$

To solve this equation, the matrix (4×3) in Eq. (13), named as matrix D has to be transformed using pseudo inverse;

$$D^+ = (D^T . D)^{-1} D^T$$

$$= \frac{1}{4} \begin{bmatrix} 1 & 1 & 1 & 1 \\ -1 & 1 & 1 & -1 \\ \frac{1}{-(L+W)} & \frac{1}{(L+W)} & \frac{1}{-(L+W)} & \frac{1}{(L+W)} \end{bmatrix} \quad (15)$$

Rearranging Eq. (13), Eq. (14) and Eq. (15), the forward kinematic equation arrangement can be obtained as;

$$\begin{bmatrix} V_X \\ V_Y \\ V_C \end{bmatrix} = \frac{R}{4} \begin{bmatrix} 1 & 1 & 1 & 1 \\ -1 & 1 & 1 & -1 \\ \frac{1}{-(L+W)} & \frac{1}{(L+W)} & \frac{1}{-(L+W)} & \frac{1}{(L+W)} \end{bmatrix} \begin{bmatrix} \omega_1 \\ \omega_2 \\ \omega_3 \\ \omega_4 \end{bmatrix} \quad (16)$$

Dynamic Modelling

Kinematic analysis is a calculation on MAVeP mobility prototype motion while dynamic modelling is a full consideration of time-varying phenomena in the interaction between motions, forces and material properties [9]. This means the dynamic modelling involves mass, friction with the floor and torque required to move the MAVeP mobility prototype. This study is important to ensure smoothness of the prototype movement and free from jerking especially when it involves carrying heavy loads or fast movement. The total kinetic energy, K is given by

$$K = \frac{1}{2}m(V_X^2 + V_Y^2) + \frac{1}{2}J_Z V_\omega^2 + \frac{1}{2}J_W(V_{\omega1}{}^2 + V_{\omega2}{}^2 + V_{\omega3}{}^2 + V_{\omega4}{}^2) \quad (17)$$

where, m is the total mass of MAVeP mobility prototype, J_Z is a MAVeP mobility prototype moment of inertia around Z axis and J_W is the wheel moment of inertia around the centre revolution. The loss energy, E is expressed in Eq. (18), where $\mu_\circ$ is the wheel friction coefficient.

$$E = \frac{1}{2}\mu_\circ\left(V_{1w}{}^2 + V_{2w}{}^2 + V_{3w}{}^2 + V_{4w}{}^2\right) \quad (18)$$

Substituting the total kinetic energy, Eq. (17) into Eq. (18) and utilizing Lagrangian equation yields

$$\boldsymbol{\tau} = \boldsymbol{M}\ddot{\boldsymbol{\theta}} + \mu_\circ\dot{\boldsymbol{\theta}} \quad (19)$$

where;

$$\boldsymbol{\theta} = \begin{bmatrix} \theta_1 \\ \theta_2 \\ \theta_3 \\ \theta_4 \end{bmatrix} \qquad \boldsymbol{\tau} = \begin{bmatrix} \tau_1 \\ \tau_2 \\ \tau_3 \\ \tau_4 \end{bmatrix}$$

$$\boldsymbol{M} = \begin{bmatrix} A+B+J_W & -B & B & A-B \\ -B & A+B+J_W & A-B & B \\ B & A-B & A+B+J_W & -B \\ A-B & B & -B & A+B+J_W \end{bmatrix}$$

$$A = \frac{mR^2}{8} \qquad B = \frac{J_Z R^2}{16(L+W)^2}$$

DC MOTOR AS ACTUATORS

Direct current (DC) motor has been selected as actuators for MAVeP mobility prototype. This type of motor is selected due to the DC character, where the motor speed is proportional to the voltage, and the DC motor is efficient for speed and position control compared to alternate current (AC) motor. Voltage control with pulse width modulator (PWM) for DC motor control produces better performance compared to frequency control for AC motor. The electric circuit of the armature and free-body diagram of the rotor are shown in Figure 11. Referring to Figure 11, R is the motor resistance, L is the motor inductance, v is the voltage supply to the system, e is electromotive, T is the motor torque, θ is the motor angular, $\dot{\theta}$ is motor angular velocity, b is motor viscous friction constant, and J is the moment inertia of the rotor. Applying Newton's law and Kirchoff's law to the motor system, the following equations can be obtained.

$$\frac{d^2\theta}{dt^2} = \frac{1}{J}\left(K_t i - b\frac{d\theta}{dt}\right) \quad (20)$$

$$\frac{di}{dt} = \frac{1}{L}\left(-Ri + V - K_e\frac{d\theta}{dt}\right) \quad (21)$$

A combination of Eq. (20) and Eq. (21) can be simulated, as shown in Figure 12. The input is voltage, V, and the output is speed, rad/s. Since the target of prototype is position control, the speed is converted to position with an integrator, as shown in Figure13. The DC motor used as the mecanum wheel actuator is SPG30E-60K. An experiment has been performed to find the motor parameter that has been used for the simulation, as shown in Table 2. These are also the parameters for SPG30E-60K motor that are used in the experiment.
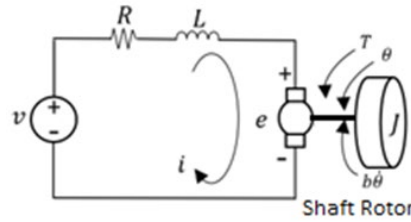
Figure11. Electric circuit of armature and rotor free-body diagram.
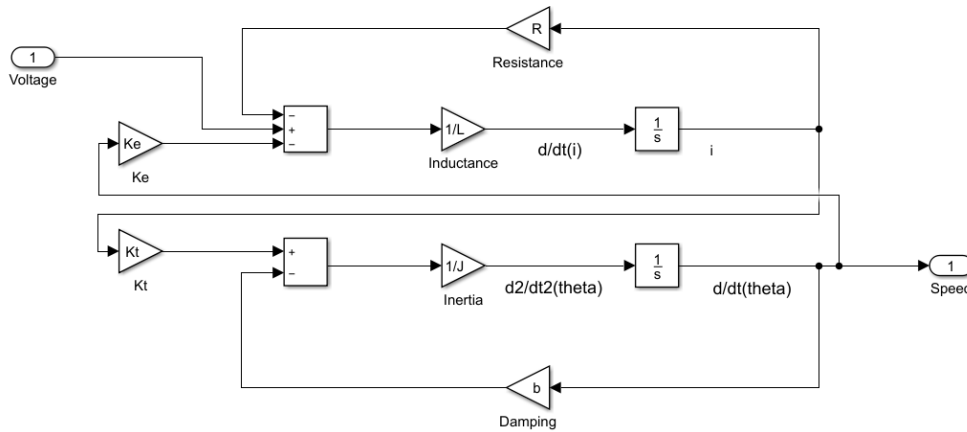
Figure 12. DC motor simulation block diagram.
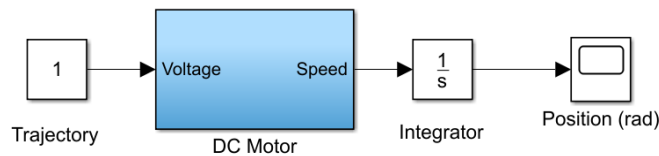
Figure 13. DC motor position control.

PID Controller Implementation

A controller has been applied to ensure the movement of MAVeP mobility prototype is accurate, repeatable and smooth. A conventional proportional-integral-derivative (PID) controller has been chosen since it is well established for DC motor positioning control and is widely used in research and industries [11-13]. The purpose of this control system is to stabilize the response and tune the DC motor to the best performance curve with minimum overshoot and no oscillation rotation from the desired trajectory to avoid jerk and vibration.

The PID controller is a feedback controller type that controls the output response in three correcting terms K_p, K_i dan K_d whose sum constitutes the manipulated variable. Defining $U_P(t)$ as the controller output, the final form of the PID algorithm is:

$$U_P(t) = K_p\, e(t) + K_i \int_0^t e^\tau d(\tau) + K_d \frac{de(t)}{d(t)} \tag{22}$$

where K_p is the proportional gain tuning parameter, K_i is the integral gain parameter and K_d is the derivative gain tuning parameter. $e(t)$ is the signal error between the system desired trajectory and the system actual output. t is the time or instantaneous time (the present) while $\int e^\tau$ is the variable of integration. Equivalently, the transfer function in the Laplace domain of the PID controller is:

$$L(s) = K_p + K_i/s + K_d\, s \tag{23}$$

Ziegler-Nichols tuning method has been applied to determine the control parameters. Table 3 shows the parameter used in the Ziegler-Nichols tuning method to obtain the control parameters as tabulated in Table 4.

P controller has been chosen as it gives the best feedback controller for SPG30E-60K. The P parameter has been tuned to give the fastest response with no overshoot and minimum settling time, as illustrated in Figure 14.

Table 2. DC motor parameters.

Symbol	Parameter	Value
J	Rotor moment of inertia	0.00317475 kgm^2
b	Damping coefficient	0.1 Nms
Ke	Electromotive force constant	1.5277 V(rad/s)$^{-1}$
Kt	Motor torque constant	13.52 NmA^{-1}
R	Resistance	12.5 Ω
L	Inductance	1.455578 H

Table 3. Ziegler-Nichols tuning method parameters.

Symbol	Value
K	1
L	0.2
T	1.8

Table 4. Controller parameters from the Ziegler-Nichols method.

Type of controller	K_p	K_i	K_d
P	9	∞	0
PI	8.1	0.667	0
PID	10.8	0.4	0
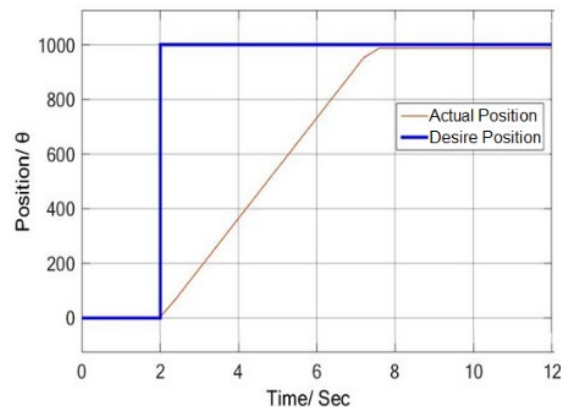
Figure14. DC motor close loop transient response after tuning.

The DC motor close loop response after tuning is shown in Figure 14. The step of the desired position is set to 1000 degrees and produces no overshoot. The settling time, 5.65 seconds is recorded, which is determined as the best-tuned response for the MAVeP mobility prototype's DC motor. The result shows that there is a 2% of error which is accepted in the experiment. These errors may come from the encoder, microcontroller or programming software itself. The tuned controller parameters are then applied to all four DC motor since all of them are of the same model.

DC Motor Calibration

There are some limitations in MAVeP mobility prototype development where the voltage supply to the DC motor is controlled with a pulse width modulator (PWM), and the rotations are captured thru the encoder. One of the most crucial limitations of the MAVeP mobility prototype is the speed of the four DC motor are not synchronous, although the inputs and controller parameters are exactly identical, as shown in Figure 15. This is because the four DC motors do not rotate at the same speed. In the first 1.25s, the speed of all wheels is lower before increasing after 1.25s. To achieve the trajectory, each DC motor response deviates from the other, as shown in the red circle. This deviation among these four wheels in the circle region demonstrates that the speed for all the motors are not the same. However, the speeds became similar after 2.2 seconds once the motors reached the desired trajectory. Therefore, a calibration procedure is performed on these four DC motors, as shown in Figure 16. The saturation block acts as a calibrator to limit the PWM. The PWM input has been programmed with 0 to 255. 0 is the fastest speed of clockwise rotation, while 255 is the fastest speed of counterclockwise rotation. Meanwhile, 128 is the center between 0 to 255, which indicates stop or no rotation. The saturation block is important to ensure that the DC motor input is within the PWM range to ensure all motors are rotated at the same speed.
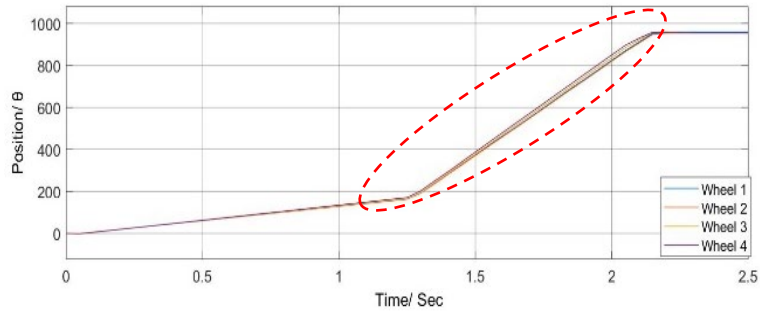
Figure 15. DC motor's response before calibration.
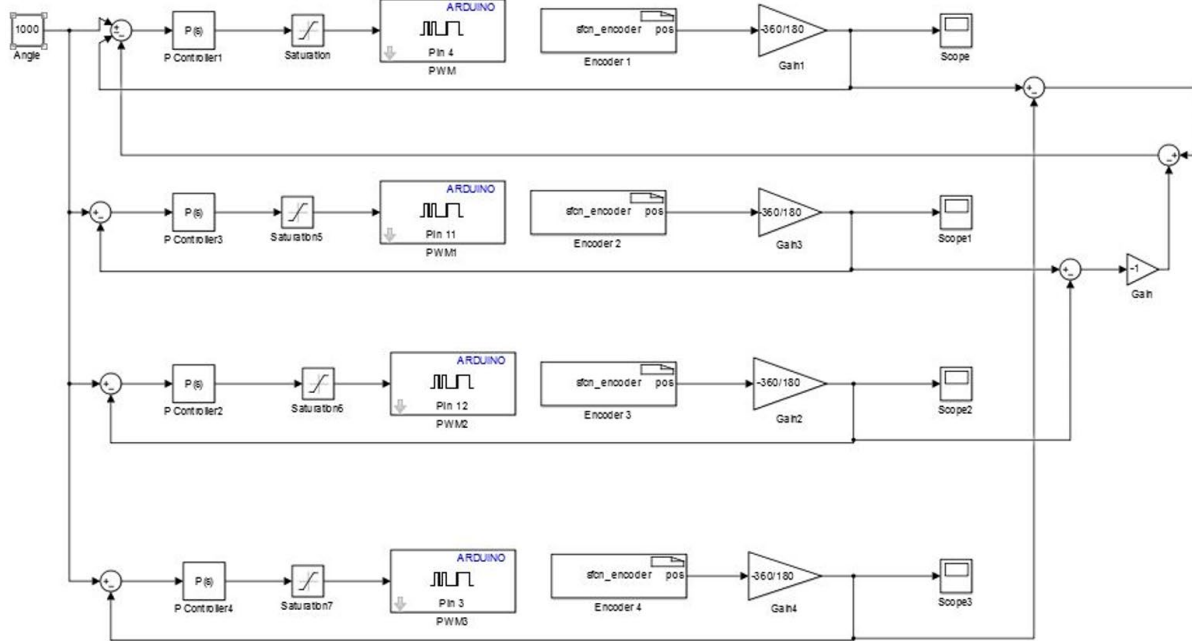
Figure 16. Calibration of DC Motor block diagram.

Although the saturation block calibration has given a huge improvement to rotation synchronization, there is still a minor error which requires further calibration. The calibration process is then continued with a comparator. The angular position rotated by motor 1 is compared to motor 4, and the angular position rotated by motor 2 is compared to motor 3. Both sets of positions are compared to each other after the direction is harmonized using gain -1. The resulting error has been sent to motor 1, and this calibration is continued until the process stops. This calibration method is effective for linear robot movement where the rotation of wheel 1 is identical to wheel 4 and the rotation of wheel 2 is similar to wheel 3 [14]. Both sets of wheels have different on its direction, while the magnitude is comparable. Figure 17 shows the response of the DC motor after calibration. The results show that the calibration performed is successful in solving the unsynchronous speed issue for the experimental set-up. Therefore, the prototype is ready for our upcoming research.
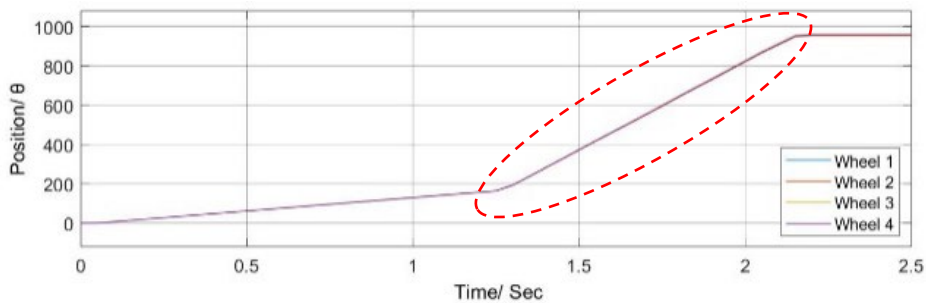
Figure 17. Response of DC motors after calibration.

CONCLUSION

This paper discusses the design and development of the lab scale of the MAVeP mobility prototype in mechanical and electrical aspects. The processes include scale down from real MAVeP, fabrication and assembly of prototype, which has been discussed in detail. The kinematic and dynamic equations of the developed MAVeP mobility prototype have been

derived, including its DC motor basic control as an actuator. The result shows that there is a 2% of error in 5.65 seconds settling time which is accepted in the experiment. This development has been completed with the calibration of four DC motor rotations by putting a saturation block as a limiter to PWM to ensure the rotations are between 0 and 255. The prototype is established for future research focusing on achieving movement accuracy and repeatability via controller development. The outcome of this prototype research will be implemented on MAVeP to increase its movement performance.

ACKNOWLEDGEMENT

REFERENCES

[1]   N. Houshangi and T. Lippitt, "Omnibot mobile base for hazardous environment," In 1999 IEEE Canadian Conference on Electrical and Computer Engineering (Cat. No.99TH8411), 1999, pp. 1357-1361 vol.3, doi: 10.1109/CCECE.1999.804891.

[2]   Data Key Communication, LLC, "ATX-series omni-directional forklift", 2006 [Online]. Available: http://www.lomag-an.org/nouveautes/20vehicules/%0Aairtrax_omnidirextional. pdf [Accessed June, 2021].

[3]   M. Göller, T. Kerscher, J. M. Zöllner, and R. Dillmann, "Obstacle handling of the holonomic-driven interactive behavior-operated shopping trolley InBOT," *Lect. Notes Control Inf. Sci.*, vol. 396, pp. 463–472, 2009, doi: 10.1007/978-1-84882-985-5_43.

[4]   U. Borgolte, H. Hoyer, C. Bühler, H. Heck, and R. Hoelper, "Architectural Concepts of a Semi-autonomous Wheelchair," *J. Intell. Robot. Syst. Theory Appl.*, vol. 22, no. 3–4, pp. 233–253, 1998.

[5]   M. A. A. N. Z. A. Mutalib and I. A.-T. Mahmood, "Modelling of mobility mechanism for motorized adjustable vertical platform (MAVeP)," In 2018 IEEE International Conference on Automatic Control and Intelligent Systems (I2CACIS), 2018, pp. 39-46, doi: 10.1109/I2CACIS.2018.8603699.

[6]   M. A. B. A. Mutalib and N. Z. Azlan, "Prototype development of mecanum wheels mobile robot: A review," *Appl. Res. Smart Technol.*, vol. 1, no. 2, pp.71-82, 2020, doi: 10.23917/arstech.v1i2.39.

[7]   S. Shahin, R. Sadeghian, P. Sedigh, and M. T. Masouleh, "Simulation , control and construction of a four mecanum-wheeled robot," vol. 2017, pp. 315–319, 2017, doi: 10.1109/KBEI.2017.8324993.

[8]   V. Alakshendra and S. S. Chiddarwar, "A robust adaptive control of mecanum wheel mobile robot: Simulation and experimental validation," *IEEE Int. Conf. Intell. Robot. Syst.*, vol. 2016-Novem, pp. 5606–5611, 2016, doi: 10.1109/IROS.2016.7759824.

[9]   R. Sadeghian *et al.*, "Control of four mecanum wheeled robot with a soft robotic glove," In 2017 IEEE 4th International Conference on Knowledge-Based Engineering and Innovation (KBEI), 2017, pp. 310–314.

[10]   Umich.edu, "DC motor speed: System modeling," 2004 [Online]. Available: ttps://ctms.engin.umich.edu/CTMS/index.php?example=MotorSpeed&section=SystemModeling [Accessed: June 2021].

[11]   M. A. Taut, G. Chindris, and D. Pitică, "PID algorithm used for DC motor control," In 2018 IEEE 24th Int. Symp. Des. Technol. Electron. Packag. SIITME 2018 - Proc., 2019, pp. 365–372, doi: 10.1109/SIITME.2018.8599230.

[12]   M. R. Ghazali, M. A. Ahmad, and R. M. T. R. Ismail, "Data-driven PID control for DC/DC buck-boost converter-inverter-DC motor based on safe experimentation dynamics," In Proc. - 2018 IEEE Conf. Syst. Process Control. ICSPC 2018, 2019, pp. 89–93, doi: 10.1109/SPC.2018.8704161.

[13]   R. K. Achanta and K. PamulaVinay, "DC motor speed control using PID controller tuned by Jaya Optimization Algorithm," In 2017 IEEE Int. Conf. Power, Control. Signals Instrum. Eng., 2017, pp. 983–987.

[14]   M. A. A. Mutalib, N. Z. Azlan, and I. A. T. Bin Mahmood, "Modelling of mobility mechanism for motorized adjustable vertical platform (MAVEP)," In Proc. - 2018 IEEE Int. Conf. Autom. Control Intell. Syst. I2CACIS 2018, 2019, pp. 39–46, doi: 10.1109/I2CACIS.2018.8603699.